THE JOURNAL OF BIOLOGICAL CHEMISTRY
Vol. 279, No. 22, Issue of May 28, pp. 23422–23430, 2004
© 2004 by The American Society for Biochemistry and Molecular Biology, Inc.
Printed in U.S.A.

The Structure of the MAPK Scaffold, MP1, Bound to Its Partner, p14

A COMPLEX WITH A CRITICAL ROLE IN ENDOSOMAL MAP KINASE SIGNALING*

Received for publication, February 13, 2004, and in revised form, March 8, 2004
Published, JBC Papers in Press, March 11, 2004, DOI 10.1074/jbc.M401648200

Vladimir V. Lunin‡, Christine Munger§, John Wagner§, Zheng Ye§, Miroslaw Cygler‡§¶, and Michael Sacher§‖

From the ‡Biotechnology Research Institute, National Research Council of Canada, Montréal, Québec H4P 2R2, Canada and the §Montreal Proteomics Network, Montréal, Québec H3A 1A4, Canada

Scaffold proteins of the mitogen-activated protein kinase (MAPK) pathway have been proposed to form an active signaling module and enhance the specificity of the transduced signal. Here, we report a 2-Å resolution structure of the MAPK scaffold protein MP1 in a complex with its partner protein, p14, that localizes the complex to late endosomes. The structures of these two proteins are remarkably similar, with a five-stranded β-sheet flanked on either side by a total of three helices. The proteins form a heterodimer in solution and interact mainly through the edge β-strand in each protein to generate a 10-stranded β-sheet core. Both proteins also share structural similarity with the amino-terminal regulatory domains of the membrane trafficking proteins, sec22b and Ykt6p, as well as with sedlin (a component of a Golgi-associated membrane-trafficking complex) and the σ2 and amino-terminal portion of the μ2 subunits of the clathrin adaptor complex AP2. Because neither MP1 nor p14 have been implicated in membrane traffic, we propose that the similar protein folds allow these relatively small proteins to be involved in multiple and simultaneous protein-protein interactions. Mapping of highly conserved, surface-exposed residues on MP1 and p14 provided insight into the potential sites of binding of the signaling kinases MEK1 and ERK1 to this complex, as well as the areas potentially involved in other protein-protein interactions.

Eukaryotic cells respond to external stimuli through any of a number of signal transduction pathways. In general, transmembrane receptors are engaged by a ligand, setting off a series of specific protein-protein interactions. These interactions transduce the signal mainly by reversible protein phosphorylation of specific tyrosine or serine/threonine residues (1, 2).

One of the first characterized and best studied signal transduction pathways is the mitogen-activated protein kinase (MAPK)[1] pathway. The kinases that make up the various branches of this pathway conform to a three-kinase module (3). One branch of the pathway responds to growth factors, leading to the activation of the MAPK kinase kinase (Raf). Activated Raf then phosphorylates and activates the MAPK kinase (MEK1/2), which, in turn, phosphorylates the MAPK (ERK1/2) (2, 3). Once activated, ERKs can phosphorylate a variety of substrates in different cellular locations (4), including the nucleus where they regulate the activity of several transcription factors (5).

Because many stimuli can lead to the activation of the MAPK pathway (6), a mechanism must exist to regulate the various branches in both a spatial and temporal fashion. One way this can be achieved is by the use of scaffolding proteins (7). It has been proposed that this class of proteins serves to prevent cross-talk among the different branches of the pathway (8), thus achieving a specific cellular response. In the Raf/MEK/ERK branch, scaffolds known to bind to MEK and ERK include KSR (kinase suppressor of Ras) (9), β-arrestin (10), and MP1 (MEK partner-1) (11). KSR is a family of large (~70–100 kDa) proteins that translocate to the plasma membrane upon receptor activation. Binding of this scaffold to the membrane may be mediated by interaction with the γ subunit of heterotrimeric G-proteins (12). In addition to this protein-protein interaction, KSR interacts with all kinases of the Raf/MEK/ERK pathway as well as with several other proteins (13–15). β-arrestin, a protein of ~45 kDa, can assemble a Raf/MEK/ERK complex (10) and binds directly to the cytosolic domain of hepta-helical transmembrane receptors (16). β-arrestin is reported to bind to activated ERK1/2, thus preventing the kinase from entering the nucleus and directing its activity toward only cytosolic substrates (17).

MP1 is unique among the other scaffolds in this branch of the pathway for several reasons. First, its size of 14 kDa is much smaller than either of the other scaffolds, perhaps restricting the number of proteins with which it can interact. Second, although the functions of ERK1 and ERK2 are equivalent in most cases and the proteins have highly similar sequences (~90% amino acid identity), MP1 favors the activation of ERK1 over ERK2 (11). Finally, MP1 has not been reported to directly interact with the MAPK kinase kinase Raf.

MP1 is localized to late endosomes via an interaction with an adaptor protein called p14 (18). Although an MP1-MEK1 interaction can take place in the absence of p14, the MP1-ERK1 interaction is greatly reduced in the absence of the adaptor

* This work was supported in part through the Genome Quebec Montreal Proteomics Network and the Genomics and Health Initiative Program of the National Research Council of Canada. The costs of publication of this article were defrayed in part by the payment of page charges. This article must therefore be hereby marked "*advertisement*" in accordance with 18 U.S.C. Section 1734 solely to indicate this fact.

The atomic coordinates and structure factors (code 1SKO) have been deposited in the Protein Data Bank, Research Collaboratory for Structural Bioinformatics, Rutgers University, New Brunswick, NJ (http://www.rcsb.org/).

¶ To whom correspondence may be addressed: Biotechnology Research Inst., National Research Council, 6100 Royalmount Ave., Montréal, Québec H4P 2R2, Canada. Tel.: 514-496-6321; Fax: 514-496-5143; E-mail: mirek@bri.nrc.ca.

‖ To whom correspondence may be addressed. Tel.: 514-496-9200; Fax: 514-496-5143; E-mail: michael.sacher@bri.nrc.ca.

[1] The abbreviations used are: MAPK, mitogen-activated protein kinase; ERK, extracellular signal-regulated kinase; MEK, MAPK/ERK kinase; aa, amino acids; PRS, proline-rich sequence; SeMet, selenomethionine; SNARE, soluble NSF attachment protein receptors.

This paper is available on line at http://www.jbc.org

protein (19). Mislocalization of p14 to the plasma membrane results in the formation of an MP1-p14 complex on this compartment, which fails to support signal transduction (19). Furthermore, both MAPK signaling and the levels of activated ERK are reduced in the absence of p14. Taken together, these results indicate that an intact and correctly localized MP1-p14 complex is required for MAPK signaling. The necessity of endosomal localization of the complex suggests the involvement of additional protein(s) in the activation of ERK.

We now report the three-dimensional structure of the heterodimeric complex between MP1 and p14 at 2.0-Å resolution. The two proteins adopt a similar fold consisting of a five-stranded β-sheet flanked by three α-helices. The interaction between these proteins is primarily mediated by an edge-to-edge association of their β-sheets, creating a seamless 10-stranded sheet. Patches of highly conserved, surface-exposed residues on both proteins are likely sites for additional protein-protein interactions. This report presents the first known structure of a mammalian MAPK scaffold protein in a complex with one of its binding partners and lays the foundation for understanding how this small scaffold protein mediates several simultaneous interactions leading to a specific cellular response.

EXPERIMENTAL PROCEDURES

Cloning of MP1 and p14—Human MP1 was obtained by PCR amplification of a cDNA using the oligonucleotide pair 5′-AAAAAA*GGATCC*GCGGATGACCTAAAGCGATTCTT-3′ and 5′-AAAAAA*GAATTC*GGTACACACTGAAACCACTGTCAGA-3′ (the BamHI and EcoRI sites used for insertion in the vector are italicized). The resulting 400-bp fragment was digested with BamHI and EcoRI and cloned into the BamHI/EcoRI site of the dual expression vector pETDuet-1 (Novagen) in which the first multiple cloning site had been modified to allow cloning, in-frame expression, and tobacco etch virus (TEV) protease cleavage of the insert (kind gift from K. Baynton). This construct is designated pJW171.

The cDNA of mouse p14 (which differs from the human ortholog at a single amino acid, S72N) was obtained by PCR amplification of a cDNA using the oligonucleotide pair 5′-AG*CATATG*CACCATCACCATCACCATCTGCGTCCCAAGGCTTTGACG-3′ and 5′-AG*GGATCC*TTATGATGCTGCTACTTGGGT-3′ (the NdeI and BamHI sites used for insertion into the vector are italicized; the His_6 tag used for purification is underlined). The resulting 403-bp fragment was first cloned into the pGEM-T vector (Promega, WI) before removing the NdeI/BamHI fragment and subcloning into the NdeI/BglII of pJW171. The resulting dual MP1/p14 expression plasmid, designated pJW173, consists of the entire coding sequence of MP1 with an additional His_8 tag and a tobacco etch virus protease cleavage site at the amino terminus (MGSSHHHHHHHHENLYFQGS), as well as the entire coding region of p14 with the addition of a His_6 tag at the amino terminus immediately following the initiator methionine.

Cell Cultures—Bacterial BL21 (DE3) cells containing the plasmid pJW173 were used to inoculate 10 ml of the autoinducible Studier ZYP-5052 defined media with 50 μg/ml ampicillin.[2] The inoculum was added to 0.5 liters of Studier ZYP-5052 medium with ampicillin, and the cells were grown for 6 h at 37 °C before reducing the temperature to 20 °C. Growth was continued for 16 h at 20 °C before cells were harvested by centrifugation at 4,500 × *g* for 10 min at 4 °C. The cell pellet was stored at −20 °C overnight.

Lemaster defined media was used for selenomethionine derivative (SeMet-labeled) protein production (20). Media containing 25 μg/ml selenomethionine and 50 μg/ml ampicillin was inoculated with a 100-ml pre-culture of the methionine auxotrophic DL41 *Escherichia coli* containing the plasmid pJW173. The culture was grown at 37 °C for 2 h, whereupon isopropyl-1-thio-β-D-galactopyranoside was added to a final concentration of 0.1 mM. After a 24-h induction at 20 °C, the cell pellet was harvested as described above.

Protein Purification—Frozen cells were thawed and resuspended in lysis buffer (50 mM Tris, pH 8.5, 400 mM NaCl, 5% glycerol, and one tablet of protease inhibitor mixture (one tablet per liter of culture). After sonication on ice, Triton X-100 (to a final concentration of 0.1%) and 2 μl of Benzonase (Novagen) were added to the lysate. The lysate was centrifuged at 45,000 rpm for 45 min at 4 °C in a type 60 Ti rotor. The supernatant was combined with 2 ml of a nickel (II)-nitrilotriacetic acid (Ni-NTA) agarose resin equilibrated in lysis buffer containing 40 mM imidazole. Binding took place on a rotating wheel for 1 h, after which the entire content was poured into a Poly-Prep Bio-Rad column. The resin was washed with 20 column volumes of wash buffer (lysis buffer containing 40 mM imidazole). Proteins were eluted with elution buffer containing 150 mM imidazole, 50 mM Tris, pH 8.5, and 300 mM NaCl. The eluted protein was concentrated and then subjected to size exclusion chromatography on a Superdex 75 column (HiLoad 16/60; Amersham Biosciences) in 50 mM Tris, pH 8.5, and 300 mM NaCl. The main peak was pooled, and the protein purity was tested by native and SDS-polyacrylamide gel electrophoresis. The protein solution was dialyzed against 10 mM Tris, pH 8.5, and 50 mM NaCl, concentrated, and used for crystallization experiments. The homogeneity of the protein solution was tested by dynamic light scattering using a DynaPro MSP-RII (Proterion Corporation, Piscataway, NJ).

The SeMet-labeled protein was purified by the same procedure. The level of selenomethionine incorporation into the protein was determined using a LC/MS-ESI mass spectrometer (Agilent 1100 Series).

Crystallization—Initial trials were performed by the sitting drop vapor diffusion method with commercially available screens purchased from Hampton Research. The drop size was 0.8 μl of mother liquor and 0.5 μl of protein sample. Optimization trials were performed by the hanging drop method. 3 μl of the protein complex (3.7 mg/ml) were mixed with 1 μl of a reservoir solution (0.1 M Tris, pH 9.0, and 14% polyethylene glycol 3350). Within 2 days, the crystals grew to a typical size of 0.01 × 0.01 × 0.05 mm. Macroseeding was used to produce larger single crystals. Medium size crystals were washed in a diluted reservoir solution and transferred into a fresh drop (ratio 3:1; protein/reservoir solution). Plates with screw caps (Nextal Biotechnologies, Montreal, Canada) were used for macroseeding. These crystals belong to the space group $P2_12_12_1$ with cell dimensions $a = 51.0$, $b = 64.1$, and $c = 73.2$ Å.

The purified SeMet-labeled protein was concentrated to 3.1 mg/ml. Crystallization trials were set up based on the optimum conditions used for native protein. Crystals for the SeMet-labeled protein grew on the surface of a native crystal seed. These crystals also belong to the space group $P2_12_12_1$, but cell dimensions changed to $a = 49.1$, $b = 64.9$, and $c = 74.5$ Å.

All crystals were cryoprotected in a solution containing 28% polyethylene glycol 3350, 12% glycerol and 0.1 M Tris, pH 8.5. Crystals were flash-frozen in a stream of N_2 gas (100 K) on a goniometer head and used for data collection.

Data Collection and Refinement—Diffraction data were collected at the X8C beamline, National Synchrotron Light Source, Brookhaven National Laboratory, using the Quantum-4 CCD detector. Three data sets at different wavelengths were collected from SeMet-labeled crystals to a highest usable resolution of 2.9 Å. Native crystals diffracted to 2 Å. Data collection statistics are shown in Table I.

The crystal structure was solved with SOLVE (21) using three data sets from SeMet-labeled crystals. All four selenium sites were found, and the mean figure of merit (FOM) for phases after SOLVE was 0.46. Density modification was performed using RESOLVE (22), and 58% of the main chain (145 residues) was automatically built. After RESOLVE, the mean figure of merit was 0.67.

This model was then manually improved and completed to ~70% of the main chain, refined as a rigid body, and used for molecular replacement against the native data set with REFMAC5 (23). Model improvement and building of the side chains were performed with ARP/WARP (24). Finally, several loops were built manually using the program O (25), and the model was refined with REFMAC5 to an R-factor of 0.201 and an R_{free} factor of 0.271. The final model contains residues 1–119 of MP1, residues 3–118 of p14, and 230 water molecules. There was one heterodimer per asymmetric unit. The model has good geometry with no outliers as shown by PROCHECK (26). The coordinates and structure factors were deposited in the Protein Data Bank with the code 1SKO. Refinement statistics are summarized in Table I.

RESULTS AND DISCUSSION

The Structure of the MP1-p14 Complex—Both MP1 and p14 are of similar molecular mass, ~13.5 kDa. They form a tight complex in the crystal (Fig. 1*A*). Whereas MP1 contains four methionines, p14 has none. Because the phasing was accomplished by the multiwavelength anomalous dispersion (MAD) method from a SeMet-substituted complex, the two molecules were easily differentiated in the experimental electron density

[2] F. W. Studier, Brookhaven National Laboratory, personal communication.

TABLE I
Data collection and refinement statistics

	Peak	Inflection	Remote	Native
Wavelength (Å)	0.979269	0.979553	0.964318	1.1
Unit cell (Å)				
a	49.1			51
b	64.9			64.1
c	74.5			73.2
Resolution range (Å)	50–2.9	50–2.9	50–2.9	50–2
(Last shell)	(3–2.9)	(3–2.9)	(3–2.9)	(2.07–2)
R_{sym}	0.089	0.096	0.086	0.07
(Last shell)	(0.330)	(0.405)	(0.414)	(0.369)
Completeness	100	100	99.2	99.6
(Last shell)	(99.9)	(100)	(99.8)	(100)
No. of reflections	29900	39205	31556	121592
Unique reflections	5665	5668	5582	16750
R-factor (R_{free})				0.201 (0.271)
No. of non-hydrogen atoms				1802
No. of water molecules				230
Average *B*-factor (Å^2), MP1 (p14)				
Protein main chain atoms				33 (39)
Side chain atoms				36 (42.5)
Water				50.2
R.m.s.d.[a] bond length (Å)				0.022
R.m.s.d.[a] bond angle (°)				1.923
Ramachandran plot				
Residues in most favorable region (%)				90.4
Residues in disallowed regions (%)				0.5

[a] R.m.s.d. is root mean square deviation.

map. Both MP1 and p14 belong to α/β fold proteins with a central β-sheet flanked on both sides by α-helices. Quite unexpectedly, the fold of both proteins is very similar (Fig. 1, *B* and *C*). This was not foreseen, because no detectable sequence homology between these two proteins was noticed. Each molecule contains a slightly convex central five-stranded antiparallel β-sheet with a strand order of $2\downarrow$-$1\uparrow$-$5\downarrow$-$4\uparrow$-$3\downarrow$. The polypeptide chain starts and ends with an α-helix (α1 and α3, respectively). These two helices are nearly antiparallel to each other and cover the convex face of the β-sheet. The concave face of the β-sheet is shielded by a long helix, α2, that runs diagonally across the strands. These three helices have a partial amphipathic character. The connections between the secondary structure elements are rather short, with somewhat longer loops connecting the α2 helix to the strands, in particular on the C-terminal side to the strand β3. The superposition of MP1 and p14 and the corresponding structure-based sequence alignment are shown in Fig. 2, *A* and *B*. These two molecules could be superimposed over 83 of 119 pairs of Cα atoms with a root mean square deviation of 1.6Å. The differences between the molecules are mainly in the conformation of the loop between helix α2 and strand β3 (Asp^{59}–Ser^{67} in MP1 and Arg^{57}–Asp^{66} in p14), which is more extended in p14, partly as a result of a shorter α2 and a shift of the C-terminal helix α3 by approximately half the helical pitch (Fig. 2*A*). The α2-β3 loop in p14 is also less well ordered in the crystal.

The sequence identity between these two proteins based on the superposition of their three-dimensional structures is only 14%. Despite very similar backbone traces and virtually the same number of residues, the surface areas of MP1 and p14 are significantly different. The MP1 molecule has an area of 6712 Å^2, whereas p14 has a larger area of 7351 Å^2, indicating more cavities and protrusions in this protein. One particular area where the surface differences are pronounced is near the β3-β4 connection and the α2 helix; in MP1 there is a cluster of aromatic residues, namely His^{44}, Phe^{50}, Tyr^{76}, Tyr^{79}, and Pro^{42}, filling the cavity (Fig. 2*C*), whereas in p14 these side chains are Thr^{39}, Ile^{47}, Cys^{75}, Gly^{78}, and Gly^{37}, resulting in a deep depression in the surface (Fig. 2*D*).

Characterization of the MP1-p14 Interface—The molecules of MP1 and p14 associate into a heterodimeric complex through an edge-to-edge (β3-β3) arrangement of their β-sheets that introduces a pseudo 2-fold symmetry (Fig. 1*A*) and creates a large 10-stranded antiparallel β-sheet. The tips of strands β2 and β3 and the short loop connecting them fold inward in both molecules, creating a canyon-like surface along the β-sheet (Fig. 1*A*). The α2 helices from MP1 and p14 extend along this canyon in an antiparallel fashion, filling it completely and providing a relatively flat surface on this side of the complex. The direction of these two helices is approximately perpendicular to the α1 and α3 helices on the other side of the sheet. The residues that form the interface are located primarily within a contiguous stretch encompassing helix α2, strand β3, and the loop following this strand. Consistent with this observation is the finding that removal of residues 62–73 in MP1, encompassing a portion of the strand β3 and the preceding loop, prevents formation of the MP1-p14 complex.[3] The side chains involved in the interactions have a predominantly apolar character (Fig. 3). The intermolecular hydrogen bonds are, to a large extent, between the backbone atoms of the two β3 strands. Only four intermolecular hydrogen bonds between side chains are formed, namely Asn^{50} . . . Gln^{60}, Tyr^{55} . . . Gln^{83}, Asp^{66} . . . Thr^{78}, and Asp^{74} . . . Lys^{70} in p14 and MP1, respectively. Several other residues are connected by water-mediated hydrogen bonds. The surface buried by the formation of the complex is 1221 Å^2 on MP1 and 1219 Å^2 on p14, corresponding to ~17% of the total solvent accessible area of each molecule. An equal surface area buried on each molecule indicates a very good surface complementarity of the two molecules at their interface.

Structural Similarities between MP1, p14, and Other Proteins—Although MP1 and p14 show no significant similarity at the amino acid level (Fig. 2*B*), the folds of these two proteins were unexpectedly found to be very similar (Figs. 1, *B* and *C*, and 2*A*). This fold is not unique to MP1 and p14. A DALI search (27) revealed similarity between MP1/p14 and the following: (i) the amino-terminal regulatory domains of sec22b (1IFQ) (28)

[3] M. Weber, personal communication.

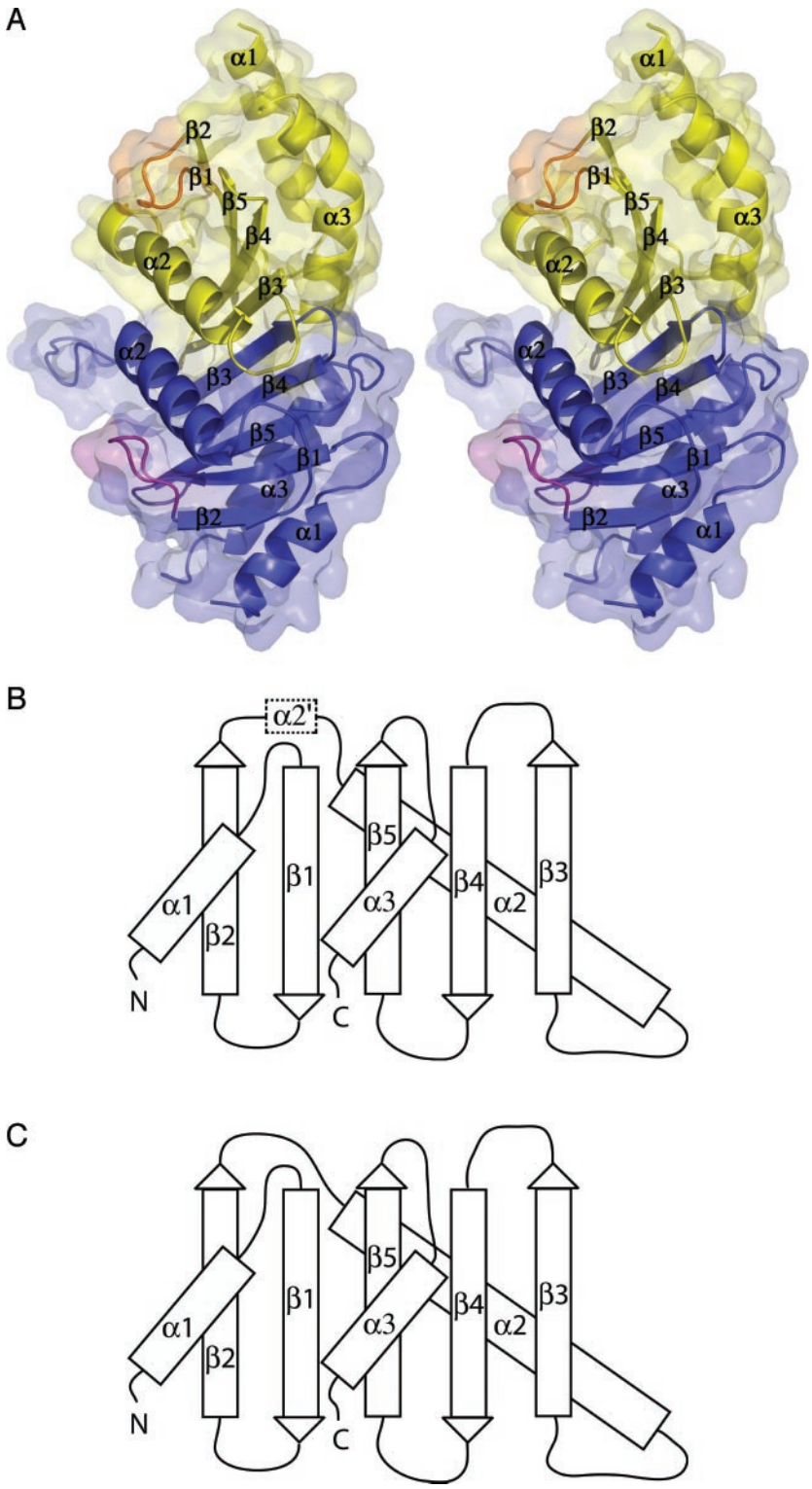

FIG. 1. **The structure of the MP1-p14 complex.** *A*, stereo view of the ribbon drawing of the MP1-p14 complex. MP1 is painted *yellow*, and p14 is painted *blue*. Superimposed on the ribbon is a semi-transparent molecular surface of the complex with the exclusion of helices α2 of both MP1 and p14. Loops lining the canyon walls are shown in *orange* (MP1) and *magenta* (p14). The figure was rendered with PyMol (DeLano Scientific; www.pymol.org). Folding diagrams of MP1 (*B*) and p14 (*C*) are shown. The five β-strands and three α-helices are shown. In MP1, α2′ indicates a five-residue helical twist from Pro^{42} to Leu^{46}.

and Ykt6p (1H8M) (29), two SNARE proteins involved in membrane fusion; (ii) the σ2 and amino-terminal portion of the μ2 subunits of the clathrin adaptor complex AP2 (1GW5) (30); (iii) sedlin (1H3Q) (31), a protein that is a component of a Golgi trafficking complex; and (iv) the Srx domain of the signal recognition particle receptor α-subunit (1NRJ) (32). All of these close structural homologs belong to the superfamily of SNARE-like proteins according to the SCOP classification scheme (33). MP1 aligns with these proteins with root mean square deviation values of 0.88–1.66Å over 47–73 C_α atoms, whereas p14 displays root mean square deviation values of 1.39–1.75Å over 54–60 C_α atoms.

The MP1 and p14 proteins are most closely related structurally to the SNARE-like superfamily of proteins involved in protein trafficking. The basis for these structural similarities is unclear, as only sec22b and Ykt6p perform similar functions. Although the direct protein partners of sedlin are unknown, the protein is a component of a multiprotein complex (34) and has been proposed to be involved in multiple protein-protein interactions (31). Similarly, the SNARE proteins are involved

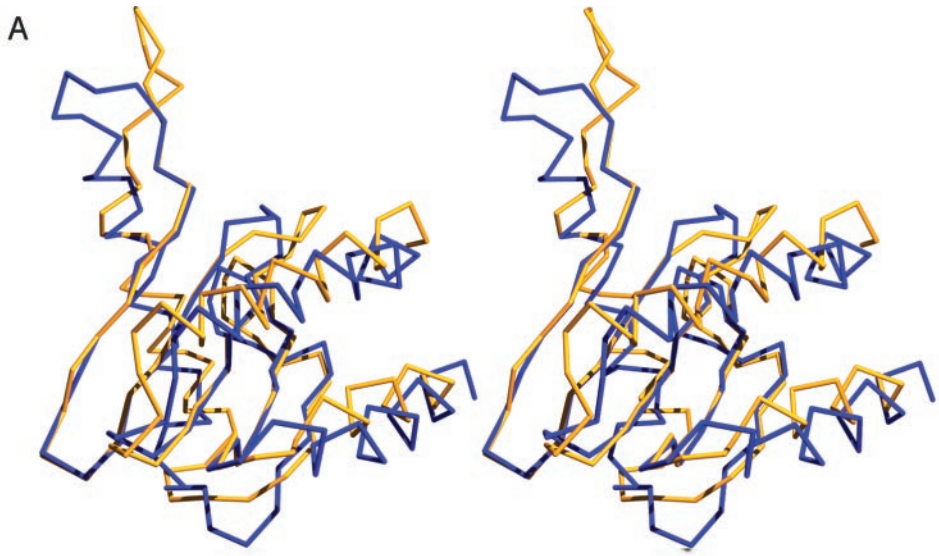

B

```
                hhhhhhhhh hhhhh    s sssssss    sssssssss          hhhh
mp1       1     GSADDLKRFL YKKLPSVEGL HAIVVSDRDG VPVIKVANDN APEHALRP--
                  .  * . *          *. .. .. . .*   .   .      .   *
p14       3       PKALTQVL SQANT--GGV QSTLLLNNEG SLLAYSGY-- -GDTDARVTA
                    hhhhhh hh      ss sssssss    sssssssss        hhhhh

                hhhhhhhhhh hhh           sssssss  sssssssss   sssssssss
mp1       49    GFLST-FALA TDQGSK-LGL SKNKSIICYY NTYQVVQFNR LPLVVSFIAS
                .. *   *      *.  .     * *.       .*        *..   *
p14       46    AIASNIWAAY DRNGNQAFNE DSLKFILMDC MEGRVAITRV ANLLLCMYAK
                hhhhhhhhhh h                 sssss   sssssssss   sssssssss

                s   hhhhhh hhhhhhhhhh
mp1       97    SSANTGLIVS LEKELAPLFE ELR
                  .   *.. .     *   .* *
p14       96    ETVGFGMLKA KAQALVQYLE EPL
                    hhhhhh hhhhhhhhh
```

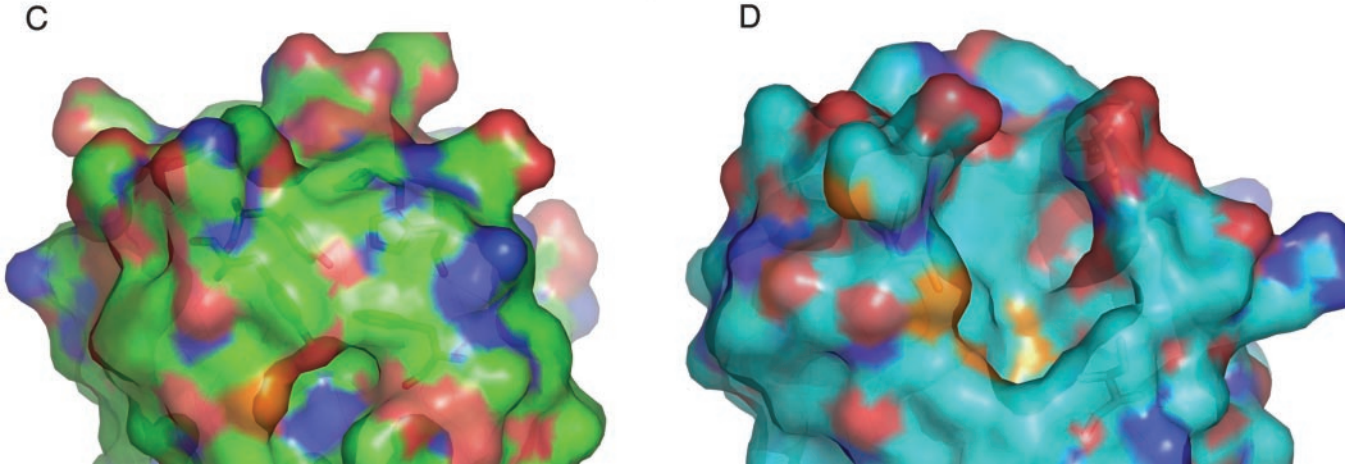

FIG. 2. **Alignment of the MP1 and p14 structures.** *A*, stereo view of the superposition of the backbones of MP1 and p14, showing their close structural similarity. The MP1 and p14 backbones are colored *blue* and *yellow*, respectively. Note the main difference between the α2-β3 loop region of both molecules, which is more extended in p14 (*top* of the figure). *B*, a structure-based sequence alignment of MP1 and p14, which indicates that there are only 17 identical residues in equivalent positions (*). The secondary structure is indicated above and below the MP1 and p14 sequences, respectively. *C*, a semi-transparent view of the surface near the aromatic cluster of MP1 (His^{44}, Phe^{5}0, Tyr^{76}, Tyr^{79}, and Pro^{42}). *D*, the corresponding surface on p14 (Thr^{39}, Ile^{47}, Cys^{75}, Gly^{78}, and Gly^{37}), viewed from the same direction. Note the deep depression in the surface of p14 by virtue of the smaller side chain residues in this region. *Panels A*, *C*, and *D* were rendered with PyMol.

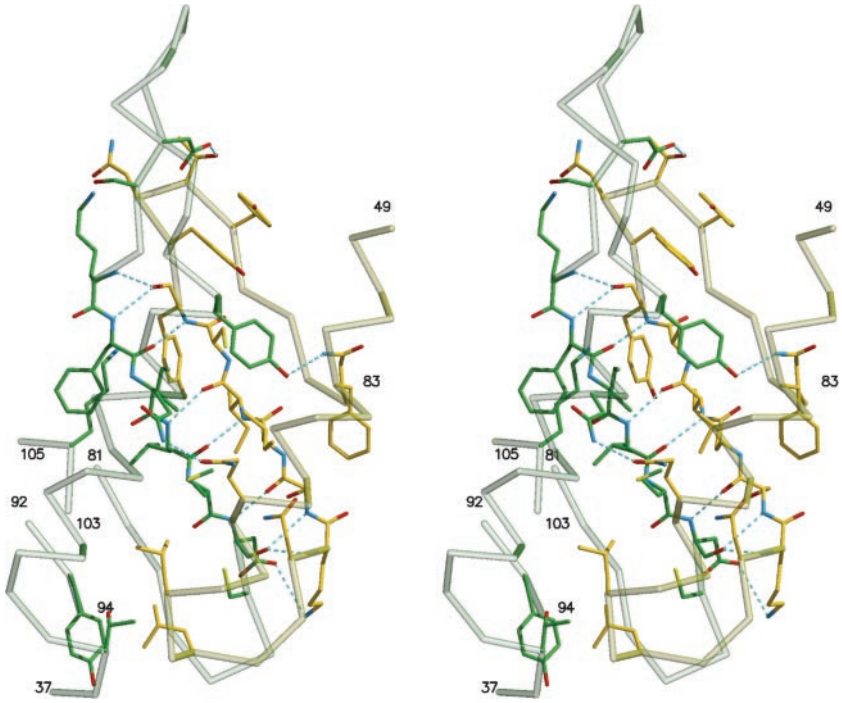

FIG. 3. **The MP1-p14 interface.** Stereo view of the MP1-p14 interface. The main chain and carbon atoms of MP1 and p14 are colored *yellow* and *green*, respectively. The side chains are colored by atom type for non-carbon atoms. *Dashed lines* show the intermolecular hydrogen bonds between MP1 and p14. N and C termini of main chain fragments are labeled with residue numbers. The figure was rendered with Molscript (53) and Raster3D (54).

in SNARE-SNARE interactions as well as in interactions with other components of the secretory pathway (35). The μ2 subunit of the AP2 complex interacts with tyrosine-based signals of various receptors, aiding in their clathrin-mediated endocytosis (36).

The fold existing in MP1 and p14 was observed in four other superfamilies, namely profilins (actin-binding proteins), GAF domain-like, PYP-like sensor domains, and the pheromone-binding domain of LuxR, and was termed a profilin-like fold in SCOP (33) or β-lactamase in CATH (37). Each of these families is characterized by a central β-sheet with five or more strands having the same connectivity as MP1, as well as helices on each side of the sheet. The specific functions of these proteins vary substantially, as they are found in photoreceptors, contractile proteins, signaling proteins, and protein transport components, but they have at least one feature in common, namely their involvement in multiple protein-protein interactions. Therefore, this fold seems to be common to proteins that have a variety of dissimilar functions but are all involved in protein-protein interactions. We therefore rationalize that this fold, encompassing roughly 120 residues, is very well suited for maximizing the possibility of diverse protein-protein interactions over a relatively small surface area.

Based on sequence analysis, p14 has been classified as a member of a much larger family of proteins named Roadblock/LC7 (38, 39), of which there are presently ~80 members in the InterPro data base (IPR004942) (40). Members of this family include bacterial, archael, and eukaryotic proteins. Several of the proteins are known to associate with dynein and are involved in various motor-related functions (38), whereas others are involved in modulating the activity of GTPases (41). Secondary structure elements indicated that family members likely contain five β-strands and three α-helices (39). Our structure determination of p14 confirmed these predictions and now provides a three-dimensional model for the other members of this family. The mapping onto the three-dimensional structure of p14 of residues that are highly conserved across all of these proteins shows that they are involved in maintaining the contacts between the β-strands and the helix α2. This type of conservation is consistent with the notion that the proteins belonging to this family perform a variety of biological functions. The only exception to this conservation pattern is either an aspartic acid or glutamic acid residue followed by an invariant glycine (Glu^{27}-Gly^{28} in p14, Asp^{29}-Gly^{30} in MP1) in the loop between strands β1 and β2. Although it has been suggested that these residues may be critical for the functions of these proteins (39), their role is not understood. From a structural viewpoint, they are located at the tip of the loops that define the canyon lined with α2 helices in the complex and are on the same side of the flat molecular surface (see Fig. 1*A*).

An exhaustive search of the NCBI data base using PSI-BLAST showed the presence of MP1-like proteins in only several organisms. These orthologous sequences were found in mouse (124 residues, 97% identity to human), rat (124 aa, 96%), fish (*Pagrus major*; 124 aa, 91%), frog (*Xenopus laevis*; 123 aa, 87%), fruit fly (*Drosophila melanogaster*; 124 aa, 45%), mosquito (*Anopheles gambiae*; 163 aa, 43%), blood fluke (*Schistosoma japonicum*; 147 aa, 33%), mold (*Dictyostelium discoideum*; 132 aa, 31%), and worm (*Caenorhabditis elegans and briggsae*; 145 aa, 20%). Strikingly, the sequence conservation from fruit fly and mosquito to man is ~45%. Such a high level of conservation during evolution in a rather small protein, including not only buried but also many solvent exposed residues, implies importance for its function and involvement in interactions with other protein(s), as is indeed suggested by experimental data (11).[3] The sequence identity drops significantly with increased evolutionary distance, yet it is still significant between worm and human sequences.

The structure of MP1 shows not only the same fold as the proteins in the Roadblock/LC7 family but also that it has the (E/D)G sequence in the loop between strands β1 and β2 (residues 29 and 30) that is characteristic for this family. When the Roadblock/LC7 family members are arranged in order of their sequence similarity to human p14, the ordered list has striking similarities to the list of orthologs of MP1. The closest sequences are from mouse and rat (99% identity), *X. laevis* (93%), *D. melanogaster* (69%), *A. gambiae* (63%) and *C. elegans* and *C. briggsae* (35%). The next sequence is from bacteria and shows only 25% identity, which is significantly lower than that

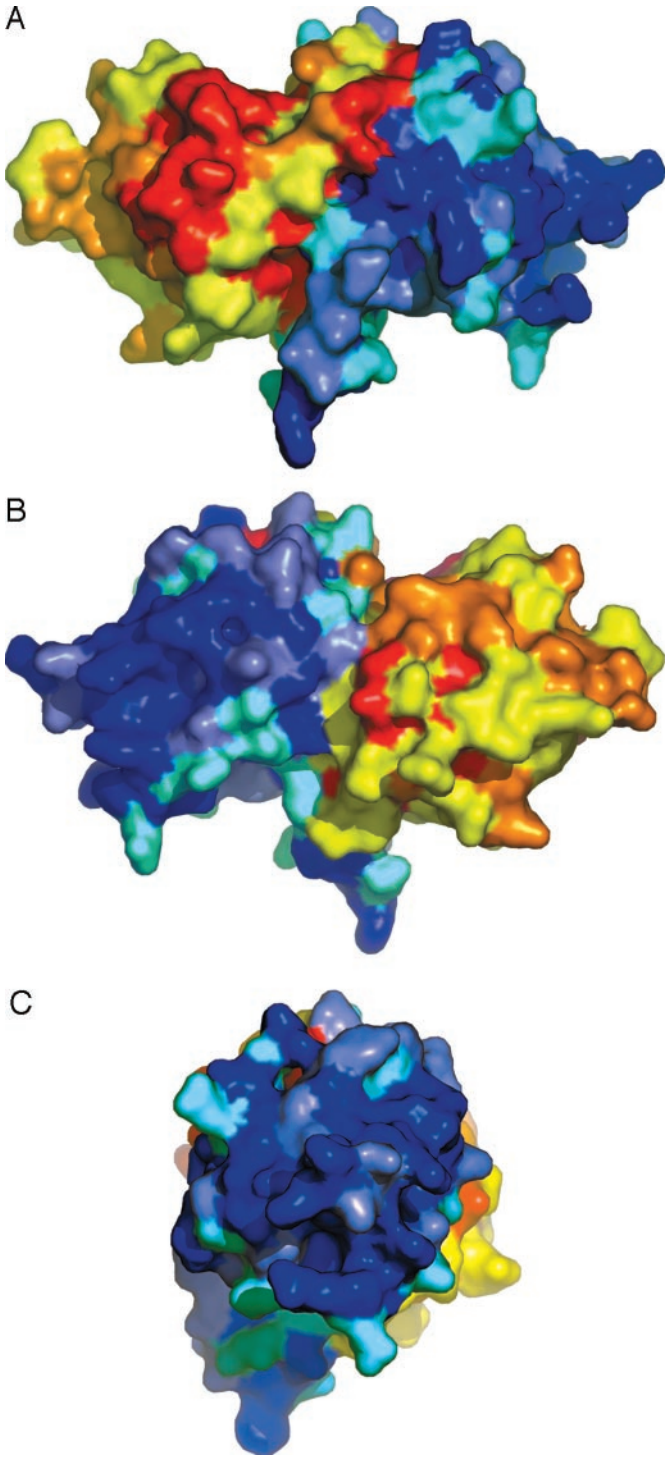

FIG. 4. **Conserved regions at the surface of MP1 and p14.** The molecular surface of the MP1-p14 complex is color-coded according to residue conservation. For MP1, identical residues in the aligned sequences of human, mouse, rat, fish, frog, fruit fly, and mosquito are colored *red*, highly conserved residues are *orange*, and the remaining residues are *yellow*. For p14, identical residues in human, mouse, rat, frog, fruit fly, and mosquito are *blue*, highly conserved residues are *slate*, and the remaining are residues are *cyan*. *A*, a view of the complex toward the face with the α2 helices from both molecules. *B*, the opposite side of the heterodimer is shown following a 180° rotation along the vertical axis. *C*, the view of p14 from the side opposite to the MP1 binding site following a 90° rotation along the horizontal axis. All panels were rendered with PyMol.

of the aforementioned eukaryotic sequences. This correspondence between the MP1 orthologs and the closest neighbors of p14 suggests that the latter form a functionally related family within the Roadblock/LC7 superfamily and that they form tight complexes with the corresponding members of the MP1 family. The absence of p14 orthologs in fish and blood fluke is likely the result of incomplete genome sequences from these organisms. Interestingly, the sequence conservation within the p14 family is substantially higher than that displayed in the MP1 family, perhaps indicating that the function and/or interactions of p14 are more highly conserved than those of MP1.

Implications for Protein-Protein Interactions—It is now established that MP1, as a MAPK scaffold, binds to several signaling kinases simultaneously (11, 19). Our determination of the structure of the MP1-p14 complex presents possible sites for kinase interaction. MP1 shows high *in vivo* specificity for the signaling kinase MEK1 as compared with the closely related MEK2. Residues 265–301 in MEK1 are part of a proline-rich sequence (PRS) that does not affect Raf-1-mediated MEK1 activation (42) but does affect the downstream activation of ERKs (42, 43). The function of MP1 as a scaffold protein is to bring MEK1 and ERK1 into close proximity, and the lack of a MEK1ΔPRS mutant interaction with MP1 (11) suggests that the PRS in MEK1 binds directly to MP1. Interestingly, although MEK1 and MEK2 share high sequence identity (80%), the PRS regions show the most divergence (56% identity), perhaps explaining the specificity of the MP1 binding seen *in vivo*.

To identify potential protein binding sites on the surface of MP1, we have analyzed the location of surface-exposed, highly conserved residues. In this analysis we considered only the organisms for which both MP1 and p14 have been identified, namely human, mouse, rat, frog, fruit fly, and mosquito. We excluded the *Caenorhabditis* homologs, as these proteins are more highly diverged from their mammalian counterparts. The conserved residues on MP1 form several large clusters, predominantly on one side of the molecule and at the interface with p14 (Fig. 4). These surfaces are composed of residues from the first loop connecting strands β1 and β2, strands β3 and β4, and the loops following helix α2 and strand β4. The conserved region on the surface of the complex (not at the interface) would be a likely site for the interaction of MP1 with both MEK1 and ERK1, keeping the two kinases in close proximity to allow for activation of the MAPK. Indeed, deletion of the sequence-divergent amino- and carboxyl-terminal helices α1 and α2 on MP1 did not interfere with MEK1 binding, whereas, in contrast, an internal deletion of residues 62–73, encompassing a well conserved region containing the loop following helix α2 and a portion of the strand β3, completely abrogated the MEK1-MP1 interaction.[3] This was not due to a complete unfolding of the MP1 protein, because this mutant was capable of interfering with MAPK activation and retained its ability to bind to ERK1,[3] indicating that the protein retains at least some of the native fold. These results, therefore, suggest that MEK1 does not bind to helices α1 or α3 and that the likely site on MP1, which binds to MEK1, is on the opposite side of the molecule defined by helix α2 and the subsequent loop region.

The sequences of p14 proteins are more conserved than those seen for MP1 (see above), and the conserved residues also form clusters on the surface of p14 (Fig. 4), indicating additional interactions or conserved function(s) for these regions. Although MP1 is the only protein currently known to bind to p14, there are reasons to suspect that other proteins might bind to it as well. First, the MP1-ERK1 interaction is strengthened in the presence of p14 (18, 19), suggesting that this protein might contribute some residues to the ERK1 binding site. Second, whereas an MP1-p14 complex can be mislocalized to the

plasma membrane (18), this mislocalized complex does not enhance MAPK signaling, (19) suggesting that other proteins on the endosomal membrane contribute to the proper functioning of the MP1-p14 complex. Specifically, the side of p14 opposite the MP1 binding site is very well conserved (Fig. 4*C*), suggesting that this end may anchor the complex to the membrane either directly or through an as yet uncharacterized protein-protein interaction or participate in additional, endosomal protein-protein interactions necessary for function.

A comparison of the MP1 structure with that of β-arrestin (44, 45), another scaffold protein in the Raf/MEK/ERK pathway, reveals two completely different structures. As mentioned above, whereas MP1 contains a five-stranded β-sheet flanked by three α-helices, β-arrestin is composed nearly entirely of β-strands with a single helix. The strands are arranged into two domains with a polar core linking them together. None of the folds in MP1 could be superimposed on β-arrestin, indicating that structural determinants alone do not reveal the mode of interaction between kinases and scaffolds.

Homodimers—An earlier report suggested that p14 could weakly self-associate to form homo-oligomers (18). However, we were unable to detect these homo-oligomers in our experimental system. Neither have we detected oligomerization of MP1 into well defined oligomers, although the presence of such oligomers has been detected in cells overexpressing MP1.[3] Perhaps the affinity between p14 and MP1 is stronger than the affinity of either p14 or MP1 for themselves. In this respect, it is noteworthy that the p14-MP1 complex was stable upon exposure to high ionic strength conditions (400 mM salt; not shown). Furthermore, the *in vivo* stability of the complex appears to be strong regardless of the local environment, as mislocalization of one component alters the localization of the other (18, 19). When recombinant p14 and MP1 were individually expressed in bacteria, solubility of these proteins was extremely poor, and only large aggregates were seen. Structurally, a p14-p14 dimer is unfavorable due to steric incompatibilities, especially between side chains of residues located on helix α2 (Ile^{51} and Tyr^{55}) and strand β3 (Lys^{69}, Met^{73}, and Met^{76}), as well as the N-terminal tip of helix α3 (Phe^{100} and Lys^{104}), regions that are crucial for the p14-MP1 interaction (see Figs. 1*A* and 3). Therefore, because p14 homo-oligomers are not structurally favorable and have not been observed *in vivo*, it seems likely that the reported p14-p14 *in vitro* interaction was simply the result of self-aggregation and is not a complex that would be found physiologically. Similarly, when an MP1-MP1 dimer is assembled, the main steric clashes are from residues in the loop between helix α2 and strand β3 (Gln^{60}–Asn^{69}). Therefore, such homodimers would also be much less stable than the MP1-p14 heterodimers.

Concluding Remarks—The functional significance of endosomal signaling is presently unclear. However, it has been suggested that the epidermal growth factor receptor (EGFR) continues to activate signaling pathways on the endosome (46–48), and signaling kinases are found on this compartment (49, 50). Although there is a growing body of evidence supporting a unique role for endosomal signaling (reviewed in Ref. 48), definitive answers are lacking, due mainly to technical difficulties in perturbing signaling from specific compartments without impacting other branches of the pathway. Interfering with protein-protein interactions specific to this portion of the pathway would be an attractive means of blocking endosomal signaling. Our characterization of the MP1-p14 interaction now makes such an endeavor possible. In addition, because many of the components of the MAPK pathway are being examined as potential therapeutic targets (51, 52), a detailed understanding of the molecular interactions of MAPK scaffolds, which assemble a functional signaling complex, may ultimately lead to better drug design.

Acknowledgments—We are grateful to Dr. Michael Weber for communicating his unpublished data and commenting on the manuscript and to Dr. Kathy Baynton for helpful discussions and critical comments.

REFERENCES

1. Pawson, T., and Scott, J. D. (1997) *Science* **278,** 2075–2080
2. Kolch, W. (2000) *Biochem. J.* **351,** 289–305
3. Garrington, T. P., and Johnson, G. L. (1999) *Curr. Opin. Cell Biol.* **11,** 211–218
4. Lewis, T. S., Shapiro, P. S., and Ahn, N. G. (1998) *Adv. Cancer Res.* **74,** 49–139
5. Brunet, A., Roux, D., Lenormand, P., Dowd, S., Keyse, S., and Pouyssegur, J. (1999) *EMBO J.* **18,** 664–674
6. Peyssonnaux, C., and Eychene, A. (2001) *Biol. Cell* **93,** 53–62
7. Morrison, D. K., and Davis, R. J. (2003) *Annu. Rev. Cell Dev. Biol.* **19,** 91–118
8. Whitmarsh, A. J., and Davis, R. J. (1998) *Trends Biochem. Sci.* **23,** 481–485
9. Roy, F., Laberge, G., Douziech, M., Ferland-McCollough, D., and Therrien, M. (2002) *Genes Dev.* **16,** 427–438
10. Luttrell, L. M., Roudabush, F. L., Choy, E. W., Miller, W. E., Field, M. E., Pierce, K. L., and Lefkowitz, R. J. (2001) *Proc. Natl. Acad. Sci. U. S. A.* **98,** 2449–2454
11. Schaeffer, H. J., Catling, A. D., Eblen, S. T., Collier, L. S., Krauss, A., and Weber, M. J. (1998) *Science* **281,** 1668–1671
12. Bell, B., Xing, H., Yan, K., Gautam, N., and Muslin, A. J. (1999) *J. Biol. Chem.* **274,** 7982–7986
13. Therrien, M., Michaud, N. R., Rubin, G. M., and Morrison, D. K. (1996) *Genes Dev.* **10,** 2684–2695
14. Yu, W., Fantl, W. J., Harrowe, G., and Williams, L. T. (1998) *Curr. Biol.* **8,** 56–64
15. Stewart, S., Sundaram, M., Zhang, Y., Lee, J., Han, M., and Guan, K. L. (1999) *Mol. Cell. Biol.* **19,** 5523–5534
16. Luttrell, L. M., and Lefkowitz, R. J. (2002) *J. Cell Sci.* **115,** 455–465
17. DeFea, K. A., Zalevsky, J., Thoma, M. S., Dery, O., Mullins, R. D., and Bunnett, N. W. (2000) *J. Cell Biol.* **148,** 1267–1281
18. Wunderlich, W., Fialka, I., Teis, D., Alpi, A., Pfeifer, A., Parton, R. G., Lottspeich, F., and Huber, L. A. (2001) *J. Cell Biol.* **152,** 765–776
19. Teis, D., Wunderlich, W., and Huber, L. A. (2002) *Dev. Cell* **3,** 803–814
20. Hendrickson, W. A., Horton, J. R., and LeMaster, D. M. (1990) *EMBO J.* **9,** 1665–1672
21. Terwilliger, T. C., and Berendzen, J. (1999) *Acta Crystallogr. Sect. D Biol. Crystallogr.* **55,** 849–861
22. Terwilliger, T. C. (2003) *Acta Crystallogr. Sect. D Biol. Crystallogr.* **59,** 45–49
23. Murshudov, G. N., Vagin, A. A., and Dodson, E. J. (1997) *Acta Crystallogr. Sect. D Biol. Crystallogr.* **53,** 240–255
24. Perrakis, A., Morris, R., and Lamzin, V. S. (1999) *Nat. Struct. Biol.* **6,** 458–463
25. Jones, T. A., Zhou, J. Y., Cowan, S. W., and Kjeldgaard, M. (1991) *Acta Crystallogr. Sect. A* **47,** 110–119
26. Laskowski, R. A., MacArthur, M. W., Moss, D. S., and Thornton, J. M. (1993) *J. Appl. Crystallogr.* **26,** 283–291
27. Holm, L., and Sander, C. (1995) *Trends Biochem. Sci.* **20,** 478–480
28. Gonzalez, L. C., Jr., Weis, W. I., and Scheller, R. H. (2001) *J. Biol. Chem.* **276,** 24203–24211
29. Tochio, H., Tsui, M. M., Banfield, D. K., and Zhang, M. (2001) *Science* **293,** 698–702
30. Collins, B. M., McCoy, A. J., Kent, H. M., Evans, P. R., and Owen, D. J. (2002) *Cell* **109,** 523–535
31. Jang, S. B., Kim, Y. G., Cho, Y. S., Suh, P. G., Kim, K. H., and Oh, B. H. (2002) *J. Biol. Chem.* **277,** 49863–49869
32. Schwartz, T., and Blobel, G. (2003) *Cell* **112,** 793–803
33. Lo, C. L., Ailey, B., Hubbard, T. J., Brenner, S. E., Murzin, A. G., and Chothia, C. (2000) *Nucleic Acids Res.* **28,** 257–259
34. Sacher, M., Barrowman, J., Schieltz, D., Yates, J. R., III, and Ferro-Novick, S. (2000) *Eur. J. Cell Biol.* **79,** 71–80
35. Söllner, T., Whiteheart, S. W., Brunner, M., Erdjument-Bromage, H., Geromanos, S., Tempst, P., and Rothman, J. E. (1993) *Nature* **362,** 318–324
36. Ohno, H., Stewart, J., Fournier, M. C., Bosshart, H., Rhee, I., Miyatake, S., Saito, T., Gallusser, A., Kirchhausen, T., and Bonifacino, J. S. (1995) *Science* **269,** 1872–1875
37. Pearl, F. M., Lee, D., Bray, J. E., Sillitoe, I., Todd, A. E., Harrison, A. P., Thornton, J. M., and Orengo, C. A. (2000) *Nucleic Acids Res.* **28,** 277–282
38. Bowman, A. B., Patel-King, R. S., Benashski, S. E., McCaffery, J. M., Goldstein, L. S., and King, S. M. (1999) *J. Cell Biol.* **146,** 165–180
39. Koonin, E. V., and Aravind, L. (2000) *Curr. Biol.* **10,** R774–R776
40. Apweiler, R., Attwood, T. K., Bairoch, A., Bateman, A., Birney, E., Biswas, M., Bucher, P., Cerutti, L., Corpet, F., Croning, M. D., Durbin, R., Falquet, L., Fleischmann, W., Gouzy, J., Hermjakob, H., Hulo, N., Jonassen, I., Kahn, D., Kanapin, A., Karavidopoulou, Y., Lopez, R., Marx, B., Mulder, N. J., Oinn, T. M., Pagni, M., Servant, F., Sigrist, C. J., and Zdobnov, E. M. (2001) *Nucleic Acids Res.* **29,** 37–40
41. Neuwald, A. F., Aravind, L., Spouge, J. L., and Koonin, E. V. (1999) *Genome Res.* **9,** 27–43
42. Dang, A., Frost, J. A., and Cobb, M. H. (1998) *J. Biol. Chem.* **273,** 19909–19913
43. Catling, A. D., Schaeffer, H. J., Reuter, C. W., Reddy, G. R., and Weber, M. J. (1995) *Mol. Cell. Biol.* **15,** 5214–5225
44. Han, M., Gurevich, V. V., Vishnivetskiy, S. A., Sigler, P. B., and Schubert, C. (2001) *Structure (Camb.)* **9,** 869–880
45. Milano, S. K., Pace, H. C., Kim, Y. M., Brenner, C., and Benovic, J. L. (2002) *Biochemistry* **41,** 3321–3328

46. Wang, Y., Pennock, S., Chen, X., and Wang, Z. (2002) *Mol. Cell. Biol.* **22,** 7279–7290
47. Sorkin, A., and Von Zastrow, M. (2002) *Nat. Rev. Mol. Cell Biol.* **3,** 600–614
48. Teis, D., and Huber, L. A. (2003) *Cell. Mol. Life Sci.* **60,** 2020–2033
49. Pol, A., Calvo, M., and Enrich, C. (1998) *FEBS Lett.* **441,** 34–38
50. Howe, C. L., Valletta, J. S., Rusnak, A. S., and Mobley, W. C. (2001) *Neuron* **32,** 801–814
51. Chang, F., Steelman, L. S., Lee, J. T., Shelton, J. G., Navolanic, P. M., Blalock, W. L., Franklin, R. A., and McCubrey, J. A. (2003) *Leukemia* **17,** 1263–1293
52. Kolch, W. (2002) *Expert Opin. Pharmacother.* **3,** 709–718
53. Kraulis, P. J. (1991) *J. Appl. Crystallogr.* **24,** 946–950
54. Merritt, E. A., and Bacon, D. J. (1997) *Methods Enzymol.* **277,** 505–524